Quantity and Quality Integrated Catchment Modeling under Climate Change with use of Soil and Water Assessment Tool Model

Ekaterini Varanou[1]; Eleni Gkouvatsou[2]; Evangelos Baltas[3]; and Maria Mimikou[4]

Abstract: This paper focuses on the regional impact of climate change on several critical water quantity and quality issues. The study area is the Ali Efenti Basin in central Greece. The soil and water assessment tool daily step conceptual model has been applied to simulate the water cycle and the nitrogen transport within the catchment. The outputs of six general circulation models have been used to perturb the time series of precipitation and temperature. For all of the scenarios a decrease in streamflow is observed and there is an increase in the magnitude of floods for certain return periods. Changes in surface water runoff influence nitrogen losses, resulting in an annual reduction of the nitrogen flux to the water body.

DOI: 10.1061/(ASCE)1084-0699(2002)7:3(228)

CE Database keywords: Catchments; Climatic changes; Water quality; Floods; Nitrogen.

Introduction

Many scientific sources are predicting global warming and climate change due to a variety of factors (Arnell 1998; Hulme et al. 1999). One of the major concerns is the assessment of the potential impacts on several critical water resources quantity and quality indicators, such as surface runoff, flood magnitude and associated risk, and nutrients. The European Union (EU) Environment and Climate Research Program sponsored a series of relevant studies. This paper presents part of the results of two EU funded projects, namely the climate hydrochemistry and economics of surface-water systems (CHESS) project and the European river flood occurrence and total risk assessment (EUROTAS) project, funded by the fourth FP-DGXII (1997–2000).

[1]Research Engineer, Dept. of Civil Engineering, Div. of Water Resources, Hydraulic and Maritime Engineering, Laboratory of Hydrology and Water Resources Management, National Technical Univ. of Athens, 5, Iroon Polytechniou, 157 73 Athens, Greece. E-mail: varanou@chi.civil.ntua.gr

[2]Research Engineer, Dept. of Civil Engineering, Div. of Water Resources, Hydraulic and Maritime Engineering, Laboratory of Hydrology and Water Resources Management, National Technical Univ. of Athens, 5, Iroon Polytechniou, 157 73 Athens, Greece.

[3]Research Engineer, Dept. of Civil Engineering, Div. of Water Resources, Hydraulic and Maritime Engineering, Laboratory of Hydrology and Water Resources Management, National Technical Univ. of Athens, 5, Iroon Polytechniou, 157 73 Athens, Greece.

[4]Professor, Dept. of Civil Engineering, Div. of Water Resources, Hydraulic and Maritime Engineering, Laboratory of Hydrology and Water Resources Management, National Technical Univ. of Athens, 5, Iroon Polytechniou, 157 73 Athens, Greece.

Note. Discussion open until October 1, 2002. Separate discussions must be submitted for individual papers. To extend the closing date by one month, a written request must be filed with the ASCE Managing Editor. The manuscript for this paper was submitted for review and possible publication on August 8, 2000; approved on October 4, 2001. This paper is part of the ***Journal of Hydrologic Engineering***, Vol. 7, No. 3, May 1, 2002. ©ASCE, ISSN 1084-0699/2002/3-228–244/$8.00+$.50 per page.

The study area is a subbasin of the Pinios River catchment, situated in the central part of Greece. It suffers from frequent and hazardous storms, and consequent flash floods, which the natural capacity of the river is inadequate to pass downstream for a large part of its length. This is mainly due to the topography of the river network, which varies from narrow passes to wide floodplains.

The Pinios River and its tributaries are sources of both irrigation and water supply. According to data provided by the Ministry of the Environment, Physical Planning and Public Works (1998), the water quality of the river network is, in general, adequate for these purposes. However, nitrate nitrogen concentrations exceeding 12 mg/L were observed during the summer months of 1990, providing inadequate water quality for the water supply. A recent report (University 1999) included the catchment in the vulnerable zones due to nitrate contamination, as nitrate concentrations exceeding 50 mg/L were detected in the groundwater. These incidents in correlation with the intensive cultivation of the agricultural areas and the considerable irrigation water needs signify the importance of the water and nutrient transport modeling in the catchment.

A conceptual daily step model, the soil and water assessment tool (SWAT), has been applied to simulate the water cycle and nitrogen fluxes. In the study area other models have been applied as well in order to estimate the hydrological effects of climate change (Mimikou et al. 2000). SWAT has some major advantages. It is a daily step model that allows for a more detailed simulation of the water cycle. It was developed to assess the long-term impacts of land use and management in large and complex watersheds, and thus provides a more holistic approach to water and nutrient yields.

The results of six climate change experiments have been used to perturb precipitation and temperature time series. Simulated, climatically changed monthly flows indicate a decrease of water yield for almost the entire year. Simulations in a daily time step give strong indications of increased flood magnitude in a climatically altered future (Knox 1993). Although the impact of climate change on water yield is well documented in the literature (Mimikou et al. 1991a,b; Mimikou and Kouvopoulos 1991; Mimikou

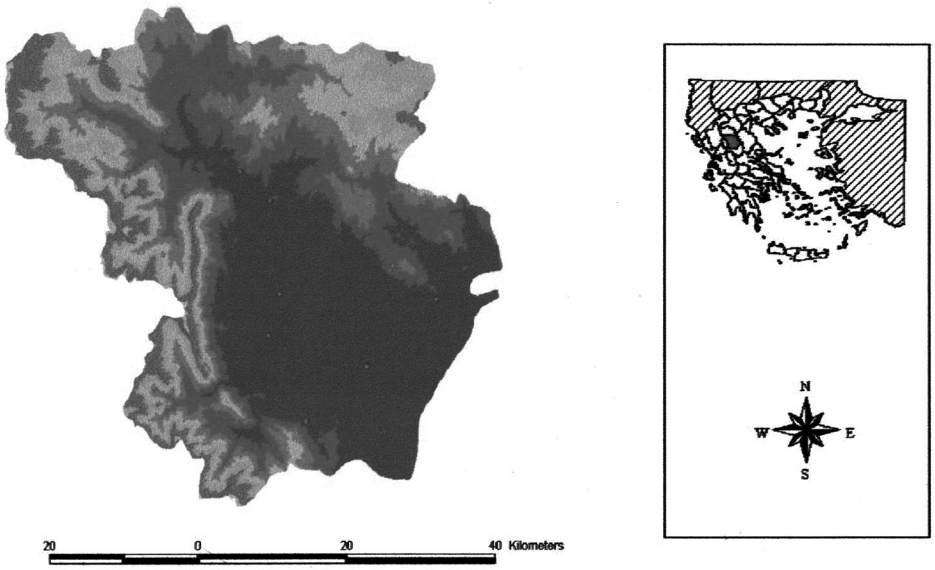

Fig. 1. Study area—Ali Efenti delineation

1995; Arnell 1998), the impact on nitrogen yields in European catchments as studied in the present paper is a quite new area of research. However, the results of this study showing decreased runoff, especially in the summer months, result in decreased nutrient release from the fields. This outcome is well in accordance with other relevant studies (Mander et al. 1998, 2000).

Study Area and Data Used

The Pinios River and its tributaries constitute the principal drainage network of the Thessaly plain, which is located in central Greece. The river originates from the Pindos range, crosses the Thessaly plain, and ends up at the Aegean Sea.

The basement of the greater area is part of the old crystalline massif, which extends to eastern and northeastern Greece. It is composed of gneiss, schists, and marbles of the Paleozoic to Triassic age. The bordering mountain ranges were uplifted during the Hellenic orogeny of the Pliocene. The Pindos range in the west consists of limestones and dolomites, associated with late Cretaceous to Tertiary flysch, and contains major ophiolithic inclusions. The eastern mountain chain is covered with Mesozoic limestones and dolomites. The depression between the mountain ranges, now the Thessaly plain, contained a shallow sea during Oligocene and Miocene times and an extensive lake in the early Pliocene epoch, in which many streams deposited alluvial fans of silt and sand (Danalatos 1992).

The study area (Fig. 1), named Ali Efenti, is a subbasin of the Pinios River network located in the northwest Thessaly district. It has a total drainage area of 2,796 km^2. The hydrometeorological characteristics of the Ali Efenti subbasin have been described in detail elsewhere (Mimikou et al. 2000). The general characteristics of the catchment are presented in Table 1. Some water quality characteristics of the Pinios River are presented in Table 2.

The required meteorological data (daily precipitation and temperature time series, average daily solar radiation for a month, and average wind speed and average relative humidity in a month) were collected from 15 stations located in the study area. Mean monthly values of these data are presented in Table 3. Observed daily flows at the basin outlet for the period 1970–1993 were used for the calibration of the water cycle of the model.

For modeling purposes, a digital elevation model derived from maps of 1:50,000 scale with a cell size of 25×25 m and a digital soil map were used. A digital land cover map by satellite imagery (CORINE vector maps) provided the spatial distribution of the different land use types. The vector maps were converted into grid maps and reclassified. The land use types in the study area are summarized in Table 4.

Agricultural production includes cereals for grain, fodder plants for seed or hay, industrial plants, vegetables, vineyards, and tree cultivations. The Ministry of Agriculture and the National Statistical Service of Greece (1997) provided the required statistical data related to the crop production, the management practices, and the fertilization application rates (data from the National Statistical Service of Greece for the years 1987–1997 were reviewed).

Table 1. General Characteristics of Study Area

Parameter	Unit	Value
Area	km^2	2,796.39
Mean elevation	m	539.73
Mean annual rainfall	mm	997
Mean annual storm runoff coefficient	—	0.428
Mean annual flow	m^3/s	39.05

Table 2. Water Quality Characteristics of Pinios River for 1989–1992 Period (Ministry 1998)

		Value		
Parameter	Unit	Minimum	Maximum	Typical
Dissolved oxygen	mg/L	8.3	14.0	—
$N\text{-}NO_3$	mg/L	0.10	12.1	2
$N\text{-}NO_2$	mg/L	0	0.21	0.01
$N\text{-}NH_3$	mg/L	0.02	0.20	0.04
P	mg/L	0.01	0.22	0.07

Table 3. Hydrometeorological Data for 1961–1990 Period

Parameter	Unit	January	February	March	April	May	June	July	August	September	October	November	December	Year
Precipitation	mm	121.3	112.9	105.4	74.1	62.7	34.9	26.1	24.0	42.6	111.3	134.4	147.4	997.0
Temperature—average	°C	3.1	3.5	6.2	8.7	13.0	15.7	17.8	17.7	14.4	10.8	6.4	4.2	10.1
Temperature—minimum	°C	0.5	0.4	2.7	4.7	8.8	11.3	13.5	13.3	11.1	7.6	3.8	1.9	6.6
Temperature—maximum	°C	4.5	5.2	8.2	10.7	14.8	16.9	18.6	18.6	15.7	12.0	7.6	5.6	11.5
Wind speed	km/h	5.0	6.5	6.8	6.8	6.5	8.3	8.6	7.2	6.5	5.8	4.3	4.0	6.4
Solar radiation	J/cm^2/day	84.2	245.7	494.7	808.1	1,090.2	1,331.7	1,339.6	1,147.5	802.7	372.1	134.8	43.9	657.9
Relative	%	78.8	76.1	71.5	66.0	62.5	57.8	54.7	56.3	64.4	74.1	77.1	79.2	68.2

Data concerning the river nitrogen loading were acquired from a monitoring station located at the basin outlet. The station has been in operation since 1988, providing measurements of nutrients and metals as well as measurements of physicochemical and microbiological parameters.

Climate Change Scenarios

A general circulation model (GCM) is a computer model representing the atmosphere, oceans, land, and icecaps. By solving mathematical equations based upon the laws of physics, a GCM simulates the behavior of the climate system.

Different GCMs not only yield different globally averaged surface air temperature changes for a given greenhouse gas concentration scenario, but also produce different spatial patterns of change in temperature, precipitation, and other variables. The greenhouse gas forcing scenarios used by all GCM experiments are expressed in terms of equivalent CO_2 concentrations. Most of these experiments use a forcing scenario of 1% per annum increase in equivalent greenhouse gas concentrations. This has been the case in the models representing the climate change scenarios used in this study.

Although the global patterns of temperature and precipitation change are broadly similar (after allowing for different climate sensitivities), the regional changes are often very different between models. The climate change scenarios used in this study are the outputs of experiments conducted with different GCMs. These models are the HadCM2 (Cullen 1993; Johns et al. 1997), ECHAM (Roeckner et al. 1996), CSIRO (Hirst et al. 1996, 1999), and CGCM (Flato et al. 1999).

The climate change scenarios from the aforementioned models refer to different time slices. In this study, climate change scenarios used from all models refer to the year 2050. Scenarios from the HadCM2 refer to 2020 and 2080 as well. Thus, two clusters of scenarios are examined. The first cluster refers to the HadCM2 scenarios with different terminal years—2020, 2050, and 2080 (Johns et al. 1997). The second cluster of scenarios refers to different GCM outputs, all for the same terminal year (2050). The climate change variables used are precipitation and temperature. Originally, these climate change variables are given in percentage change for precipitation and degrees Celsius change for temperature. These changes have been applied to the climate of the recent past (specifically 1961–1990) in order to obtain the climatically changed precipitation and temperature time series according to the scenarios. The 30 year mean monthly average values for the baseline and the scenarios regarding precipitation and temperature are presented in Figs. 2(a and b) and 3(a and b).

Evolution in temperature is quite consistent for the two clusters of scenarios. Temperature increase is suggested from all scenarios and for all of the terminal years. As expected, the highest increase of temperature is simulated by the HadCM 2080 scenario and reaches 5.3°C in September. The HadCM 2020 scenario simulates the lowest increase of temperature in May (1.1°C). In the second cluster of scenarios with the terminal year 2050, the ECHAM gives the highest increase (3.8°C) in July. The lowest increase in temperature is simulated by the HadCM, with 1.7°C in November. Changes in precipitation are mainly reductions for both clusters of scenarios and for most months. Some increases are also observed, mainly in January and February. In general, the magnitude of change is different from one scenario to the other. Reduction in precipitation can be as high as 100% for some scenarios in the summer months.

Table 4. Land Use Distribution in Ali Efenti Catchment

Land use	Area (km^2)	Percent
Broad leaved forest	243.85	8.72
Coniferous forest	184.56	6.60
Mixed forest and sclerophyllous vegetation areas	382.27	13.67
Moors, heathland, and natural grasslands	833.04	29.79
Nonirrigated arable land	537.19	19.21
Permanently irrigated land	573.26	20.50
Others	42.22	1.51
[Total]	2,796.39	100

Soil and Water Assessment Tool Model

The SWAT is a physically based model used to simulate the hydrological cycle and its influence on the quantity and quality of the water and sediments (Arnold et al. 1994). The model integrates the functionalities of several other models, allowing for the simulation of climate, hydrology, plant growth, erosion, nutrient transport and transformation, pesticide transport, and management practices. SWAT can also simulate in-stream processes with respect to sediments, nutrients, and pesticides. It is considered to provide a complete catchment system representation, as it has the ability to describe all of the physical activities taking place in a catchment.

SWAT operates under a geographic information system (GIS), based on the ArcView platform. SWAT integrates ArcViewGIS with water resources modeling, providing a powerful tool for addressing hydrology issues in space and in time.

The model has been described extensively in the literature (Krysanova et al. 1998; Arnold et al. 2000). Herein some of the basic model modules are briefly discussed.

Climate in Soil and Water Assessment Tool

Basic inputs of the model are daily time series of precipitation, minimum and maximum temperature, average daily solar radia-

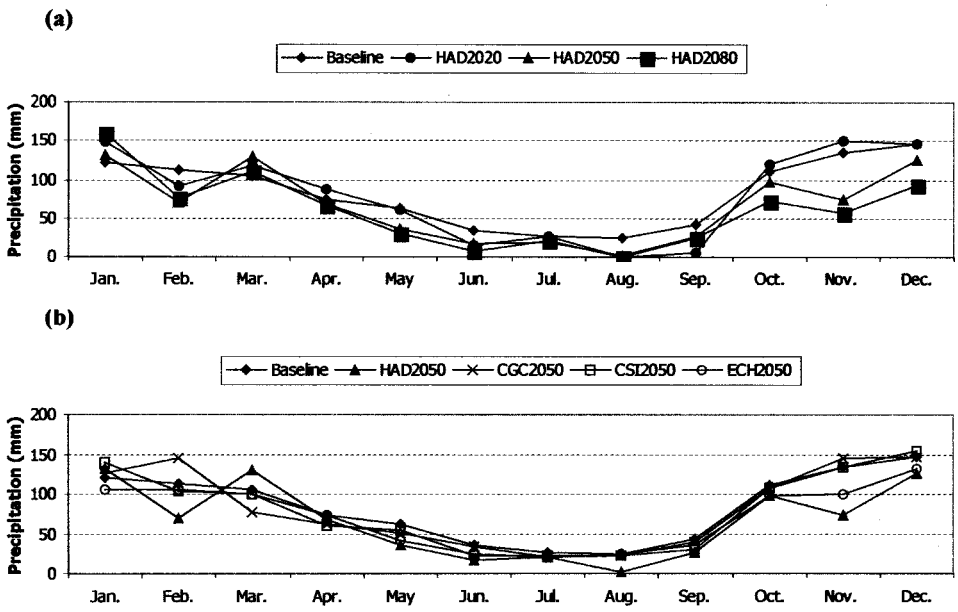

Fig. 2. Thirty-year mean monthly precipitation averages: (a) baseline and first cluster of climate change scenarios; (b) baseline and second cluster of climate change scenarios

tion for a month, average wind speed, and average relative humidity in a month. Missing precipitation data are generated by a first-order Markov chain model. Solar radiation and temperature data are generated from a normal distribution and an incorporated continuity equation. Daily mean wind speed and daily average relative humidity are always generated by incorporated models (Neitsch et al. 1999).

Hydrology in Soil and Water Assessment Tool

Surface runoff is estimated by a modification of the Soil Conservation Service (SCS) curve number method, while peak runoff rates are predicted from a modification of the rational method. Subsurface flow is moved downward through the soil layers with a rate predicted by the soil layer hydraulic conductivity, ending up

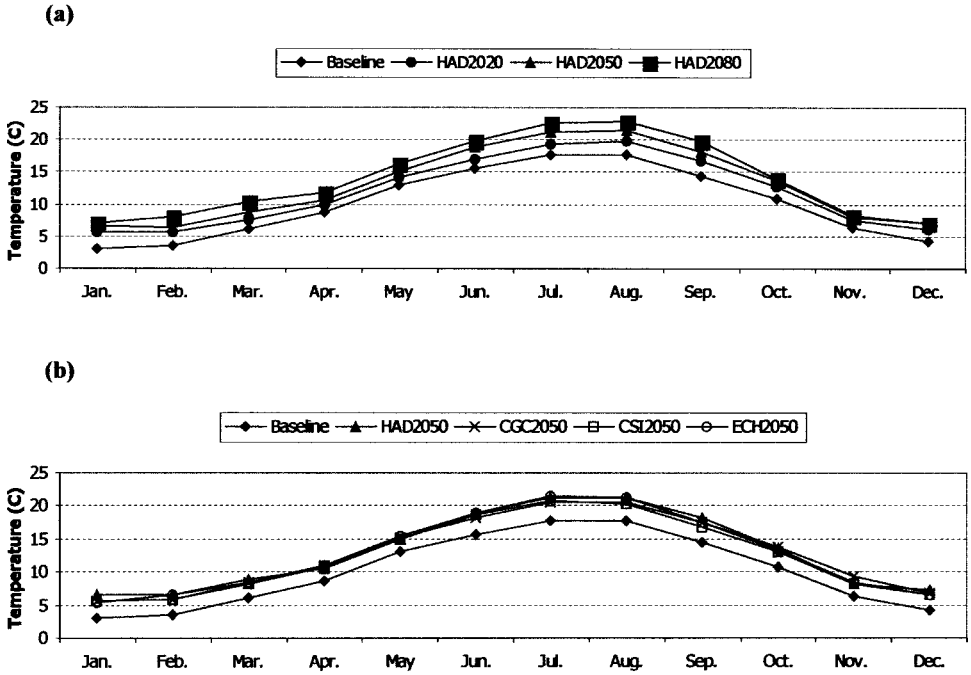

Fig. 3. Thirty-year mean monthly temperature averages: (a) baseline and first cluster of climate change scenarios; (b) baseline and second cluster of climate change scenarios

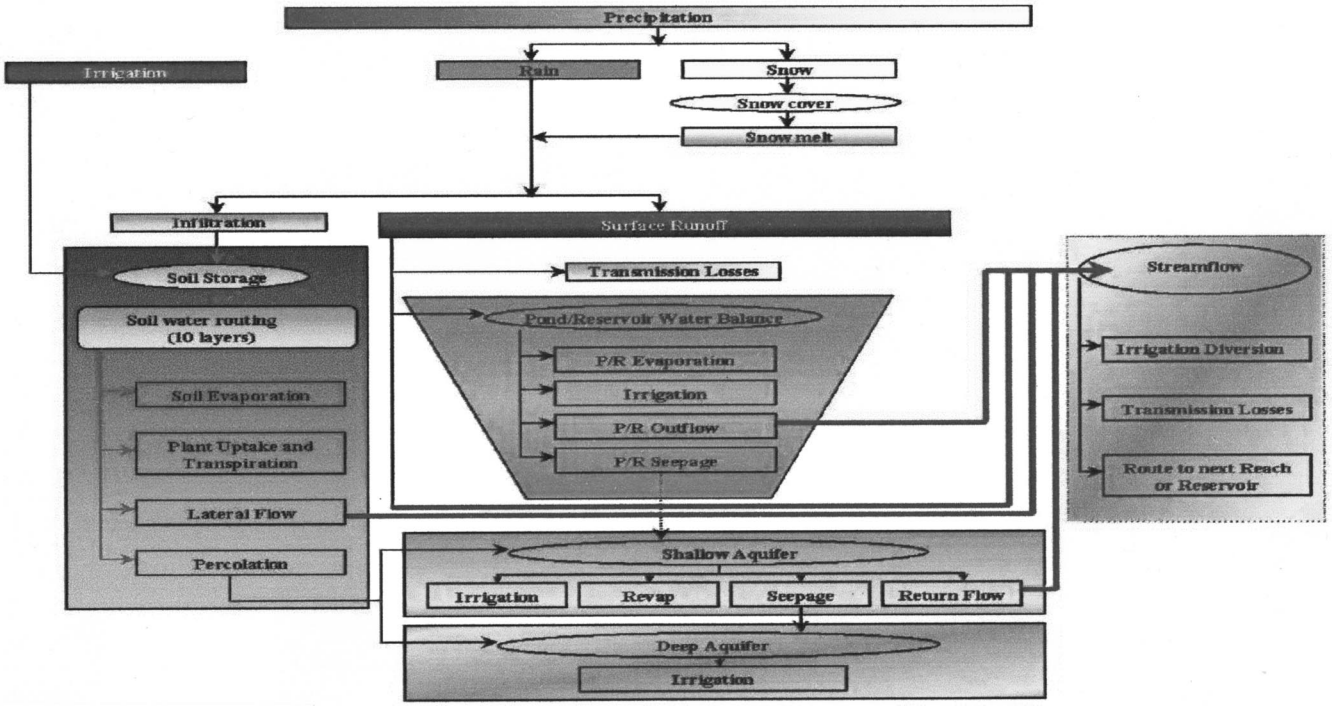

Fig. 4. Schematic of pathways available for water movement in soil and water assessment tools (Neitsch et al. 1999)

in the shallow or deep aquifer. Lateral flow contributing to the streamflow is also simulated by the model. Return flow from the shallow aquifer also contributes to the streamflow, while return flow from the deep aquifer contributes to streams outside the watershed (Neitsch et al. 1999). The available pathways for water movement as modeled in SWAT are presented in Fig. 4.

Potential evapotranspiration can be calculated with the following three different methods: the Penman-Monteith method, the Hargreaves method, and the Pristley-Taylor method. Potential evapotranspiration is used for the estimation of potential soil water evaporation and plant transpiration. Soil type and vegetation are also used to evaluate evapotranspiration. Actual soil evaporation is estimated by using exponential functions of soil depth and water content. Sediment yield is estimated with the modified universal soil loss equation (MUSLE), taking into account the predicted surface runoff volume and peak runoff rate, along with other factors such as soil erodibility and crop management.

Nitrogen in Soil and Water Assessment Tools

SWAT divides the N cycle in the soil into two parts. The first part is associated with organic N transport and transformations, while the second part is associated with inorganic N transport and transformations (Fig. 5).

Organic nitrogen comes from fresh plant residue, soil humus, and fertilizers (manure). Plant residues decompose and enrich the fresh organic N pool, while N associated with soil humus is divided into the active (readily mineralizable) and stable pool. SWAT simulates a flux from the stable to the active pool, whereas the active pool is subject to mineralization. Mineralization is calculated as a function of soil water content, temperature, and the available organic N in the pool. Mineralization also occurs in the fresh organic nitrogen pool, and is calculated as a function of crop residue, temperature, and soil water content and temperature (Neitsch et al. 1999).

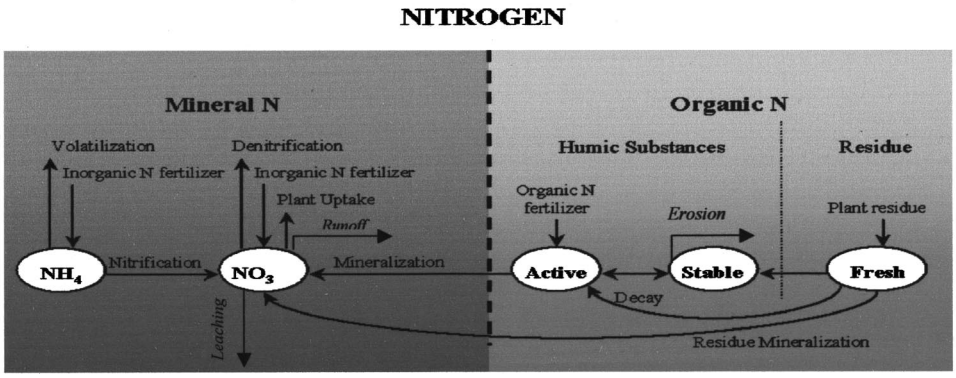

Fig. 5. Modeling flowchart for nitrogen cycle in soil and water assessment tools [adapted from Neitsch et al. (1999)]

Denitrification takes place in the nitrate pool and is a flux of nitrogen to the atmosphere. SWAT calculates denitrification as a function of soil water content, temperature, organic carbon content, and available mineral N.

Nitrogen plant uptake is calculated as the difference between the actual concentration of nitrogen in the plant and the optimal concentration. It is a function of the type of plant growing and the stage of the growing season. In the case of legumes (e.g., alfalfa), if the soil cannot meet the daily N demand, the deficit is attributed to N fixation. SWAT allows for a nitrogen contribution from rainfall, estimated by the amount of rainfall and an average N concentration of 8 ppm for all of the rainfall events.

The model can simulate the different management practices taking place in each hydrologic response unit, regarding the planting, harvesting, tillage operations, and irrigation and fertilizer applications. The user can specify the amount of fertilizer/manure applied, the fraction of organic nitrogen in the fertilizer, the fraction of inorganic N ($N\text{-}NO_3$ and $N\text{-}NH_4$), the fraction of inorganic N applied as ammonia, as well as the soil layer that the fertilizer is applied at. Depending on the type of fertilizer applied, N is added to the appropriate nitrogen pool (active pool, $N\text{-}NO_3$ pool, $N\text{-}NH_4$ pool).

Nitrate can be removed from soil with water flow. SWAT calculates the amount of $N\text{-}NO_3$ lost in runoff, considering the processes taking place in the topsoil layer as a function of $N\text{-}NO_3$ concentration in the top layer and the total water volume lost from that layer. Surface runoff, lateral flow, and percolation volumes determine the mass of $N\text{-}NO_3$ lost in surface and subsurface flows, as well as the amount of $N\text{-}NO_3$ leaching. Organic N transported with sediments is calculated as a function of organic N in the topsoil layer, the sediment yield, and the ratio of organic nitrogen concentration attached to the sediments divided by the organic nitrogen concentration in the soil.

Climate Change Impacts on Catchment Water and Nitrogen Yield

The growing concern for some environmental issues in a river basin (water availability, good water quality, flood mitigation) under a variable and uncertain climate underscores the need to study the regional effects that climate change has on water resources. The methodology used in this study in order to address the impacts of climate change on water resources consists of estimating the changes on the water balances, the changes on flood magnitude for certain return periods, and the changes on nitrogen losses.

Water Yield

The model was calibrated against the 1970–1993 period of observed daily runoff at the basin outlet. For the simulation, the model requires the first six to seven years as a warm-up period in order to account for the initial conditions. A number of parameters needed to be adjusted during the calibration. The model proved to be more sensitive while adjusting the SCS runoff curve number for moisture condition II and a number of groundwater parameters. Some of these parameters, their usual ranges, and the values giving the best fit can be seen in Tables 5 and 6. The monthly calibration was quite satisfactory, with an efficiency coefficient (Nash and Sutcliffe 1970) of 0.81 (Fig. 6; warm-up period has been neglected). Usually, such a coefficient ranges between 0 and 1, with 1 indicating a perfect fit. Values around 0.7 are fairly good for the monthly simulations (Krysanova et al. 1998). Daily calibration, as expected, had a lower efficiency number, equal to 0.62.

Table 5. Calibration Parameters, Ranges, and Values: Soil Conservation Service Runoff Curve Numbers (CN)

Land use	CN II	Typical value
Pasture	71	69
Range	73	69
Urban	82	78
Forest (deciduous)	68	66
Forest (evergreen)	60	55
Forest	62	60
Agricultural land	79	77

Annual daily maxima were sampled and the Gumbel maximum distribution had been fitted. Afterward, the 10, 20, 100, and 1,000 year floods had been estimated, which were then used as the base for addressing the change in flood magnitude.

The perturbations of the baseline daily time series (1961–1990) were carried out in a simple manner. The provided change in temperature (°C) in each month was added to the baseline temperature of all days of that month, and the baseline daily precipitation of each month was multiplied by the provided change in precipitation (%) in that month. Base runs of the model refer to the 1961–1990 period and account for the flows under the current climate. Further runs of the model using the perturbed precipitation and temperature resulted in the climatically changed flows, which were then compared against the base flows for the estimation of the changes in the monthly water balances and the changes in the flows of different return periods.

Nitrogen Yield

Having calibrated the hydrological part of the model, calibration of the total and nitrate nitrogen was made against nitrogen loads also observed at the basin outlet. The ''robust approach'' of calibration (Krysanova et al. 1998) was followed, in order to overcome a series of uncertainties or assumptions, as follows:

- Spatial crop distribution; approximation in the agricultural land use map,
- Parameters concerning some soil profiles,
- Actual quantities of fertilizers applied,
- Lack of information about the livestock in the study area,
- Lack of surface water flow and sediment load measurements, and
- In-stream processes such as nitrogen removed by sedimentation or macrophyte uptake and denitrification (Skop and Sørensen 1998) were neglected.

Table 6. Calibration Parameters, Ranges, and Values

Parameter	Value	Typical range
(a) Groundwater Parameters		
Alpha factor	0.600	0.0–1.0
Groundwater delay	100 days	—
Revap coefficient	0.05	0.02–0.20
Deep aquifer percolation fraction	0.700	0.0–1.0
(b) Other Basin-Specific Parameters		
Soil evaporation compensation factor	0.2	0.0–1.0
Sur-lag (concentration time)	19 h	—

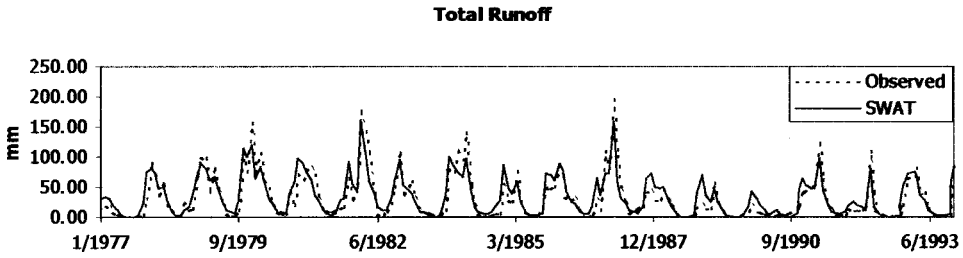

Fig. 6. Water flow simulation (monthly averages) for 1977–1993 period

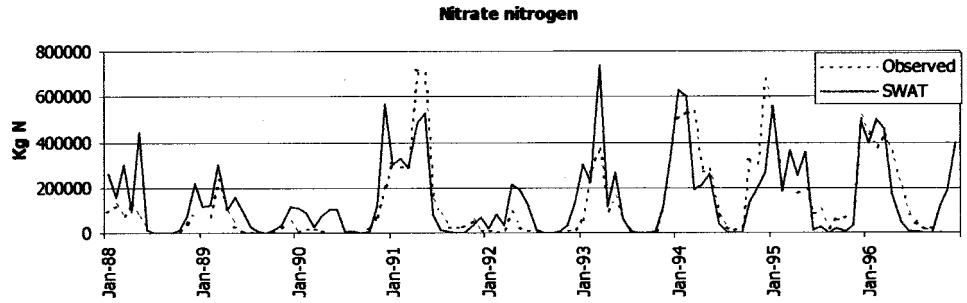

Fig. 7. Nitrate nitrogen simulation (monthly averages) for 1988–1996 period

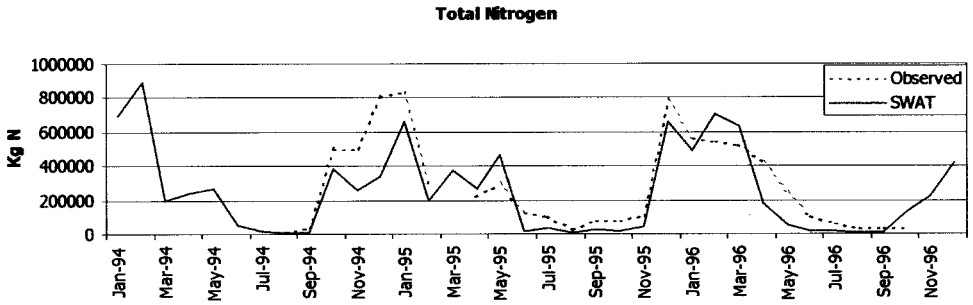

Fig. 8. Total nitrogen simulation (monthly averages) for 1994–1996 period

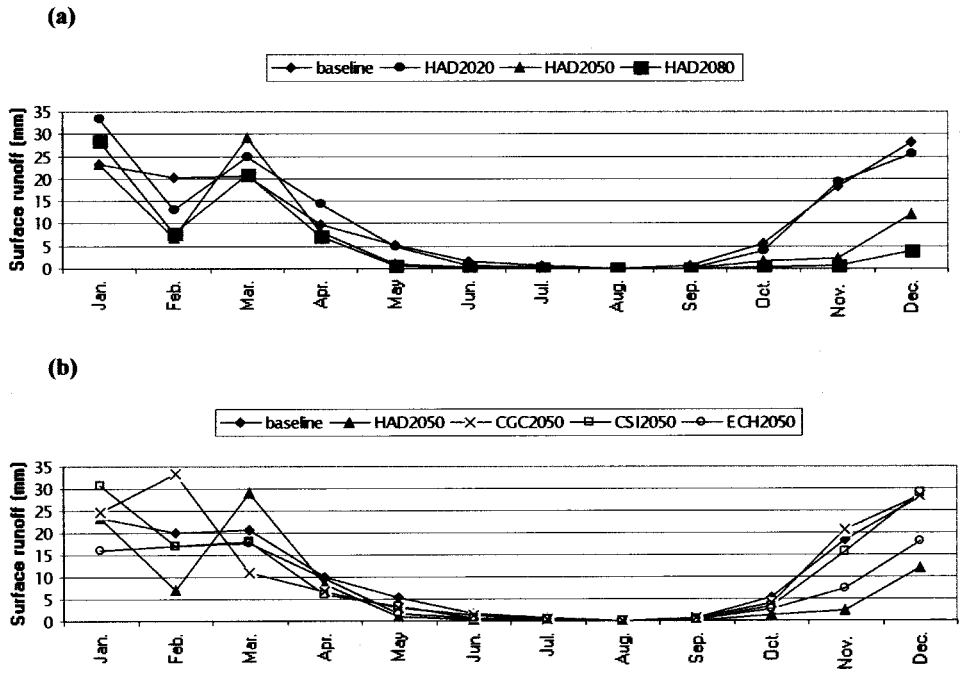

Fig. 9. Mean monthly surface flow: (a) baseline and first cluster of climate change scenarios; (b) baseline and second cluster of climate change scenarios

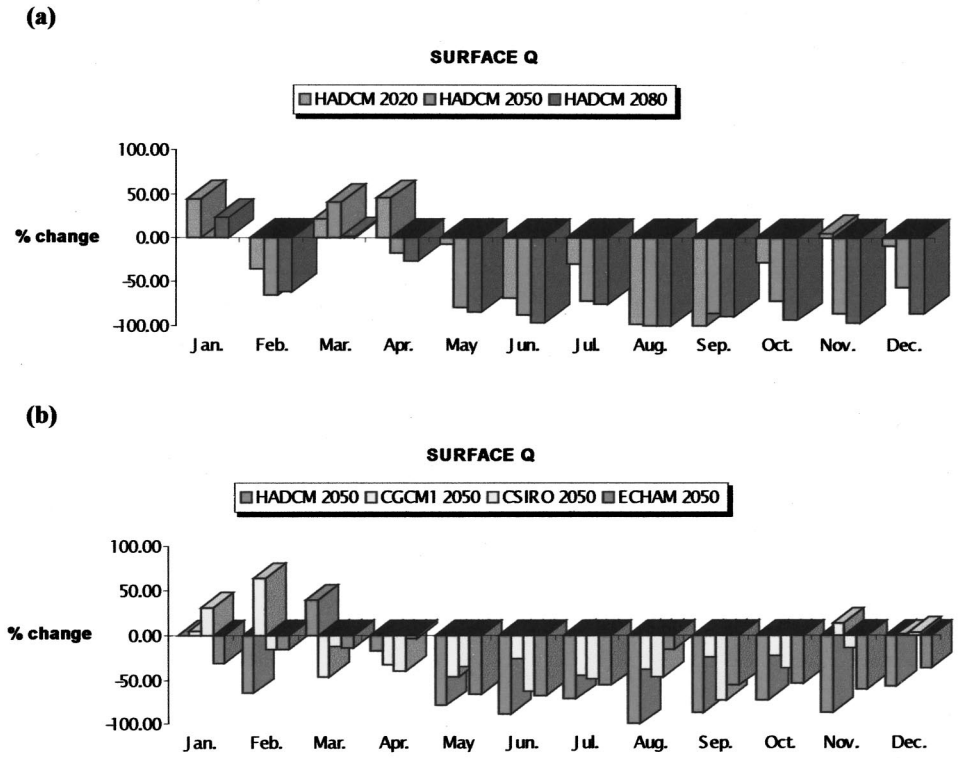

Fig. 10. Percentage changes of mean monthly surface flow: (a) first cluster of climate change scenarios; (b) second cluster of climate change scenarios

When using a robust approach in nitrogen modeling, the model flowchart of nitrogen dynamics in the soil is simplified, including only the main forms of nitrogen and the flows between them. Additionally, some certain requirements regarding the modeling procedure and interpretation of the results should be met. The hydrological module should be tested and validated in advance, and the results must be interpreted in the first place qualitatively, showing trends, qualitative differences, etc., and not as ''exact'' predictions.

Figs. 7 and 8 present some selected periods of the simulated and observed nitrate and total nitrogen loads, respectively. Seasonal trends are simulated quite well, though for the simulations,

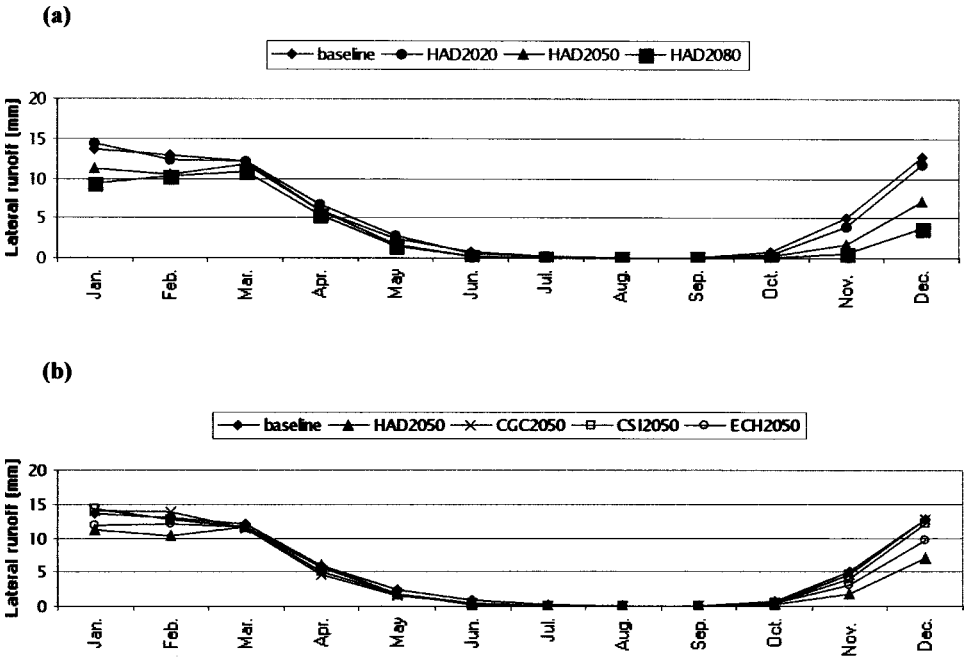

Fig. 11. Mean monthly lateral flow: (a) baseline and first cluster of climate change scenarios; (b) baseline and second cluster of climate change scenarios

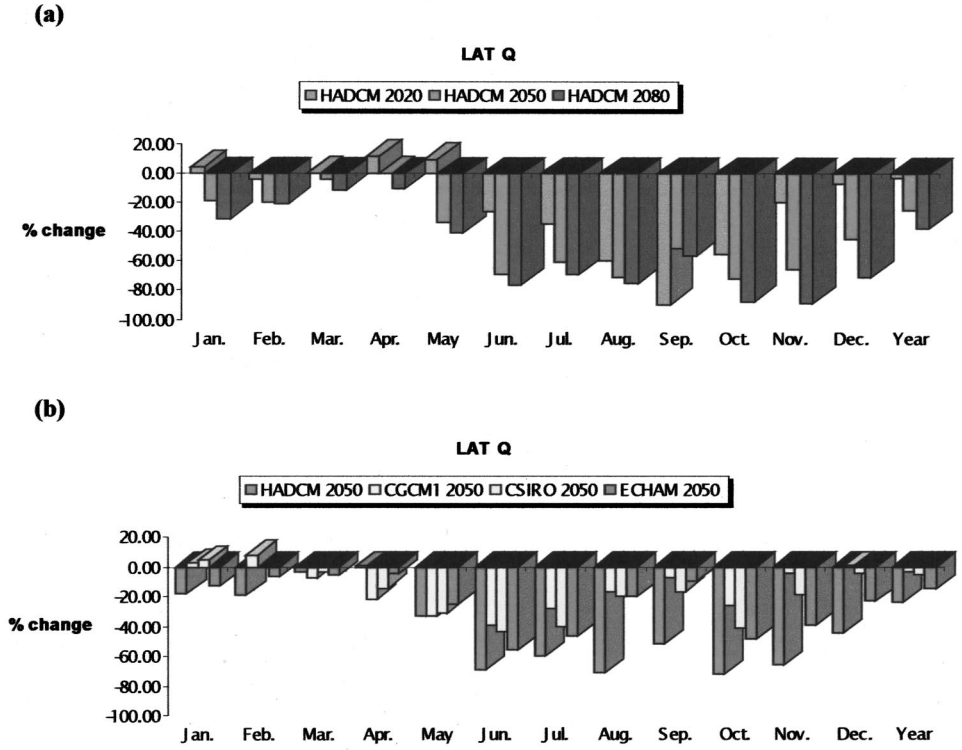

Fig. 12. Percentage changes of mean monthly lateral flow: (a) first cluster of climate change scenarios; (b) second cluster of climate change scenarios

the in-stream model of SWAT was not used. Further research work will link SWAT with R-QUAL, an in-stream model developed by NTUA (Mimikou et al. 1999a, 2000) in order to simulate the in-stream nitrogen transformations and retention, and thus provide more reliable results.

After the model was calibrated under the current climate conditions, further runs were performed to account for climate change as introduced by the climate change scenarios. For these runs, the land use map and management practices were considered to be the same. Temperature and precipitation time series as predicted by the climate change scenarios were the new input for the model.

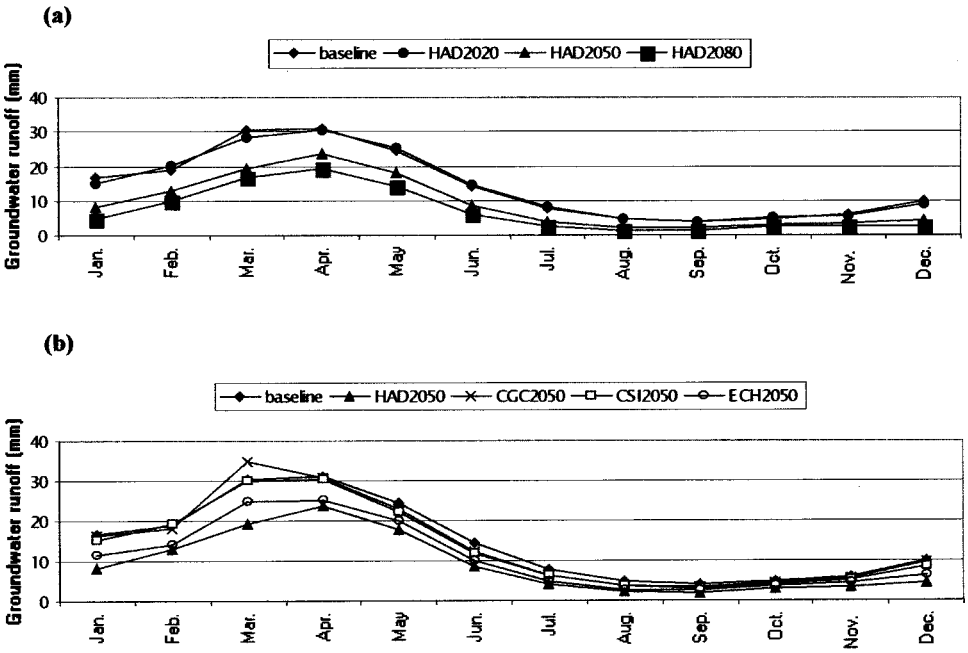

Fig. 13. Mean monthly groundwater flow: (a) baseline and first cluster of climate change scenarios; (b) baseline and second cluster of climate change scenarios

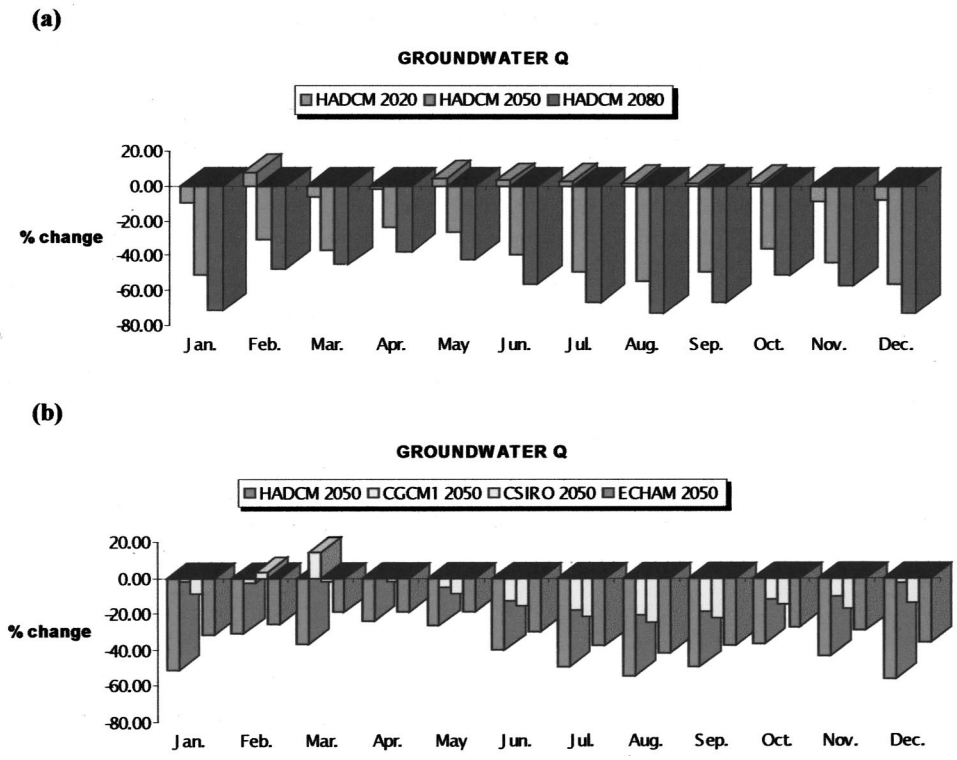

Fig. 14. Percentage changes of mean monthly groundwater flow: (a) first cluster of climate change scenarios; (b) second cluster of climate change scenarios

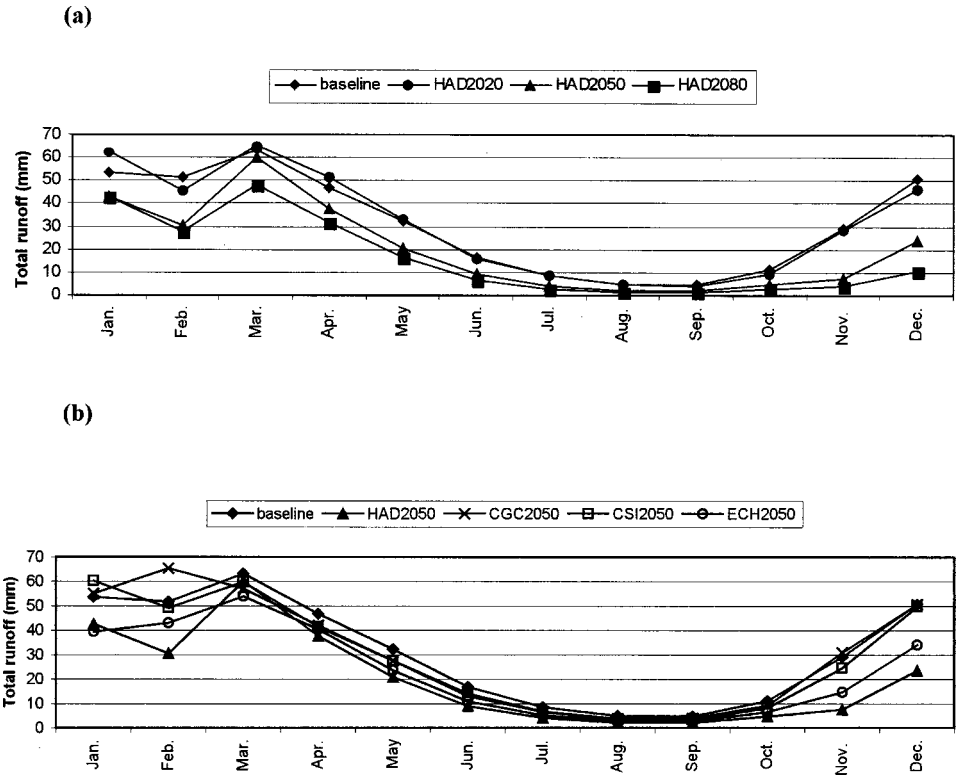

Fig. 15. Mean monthly total runoff: (a) baseline and first cluster of climate change scenarios; (b) baseline and second cluster of climate change scenarios

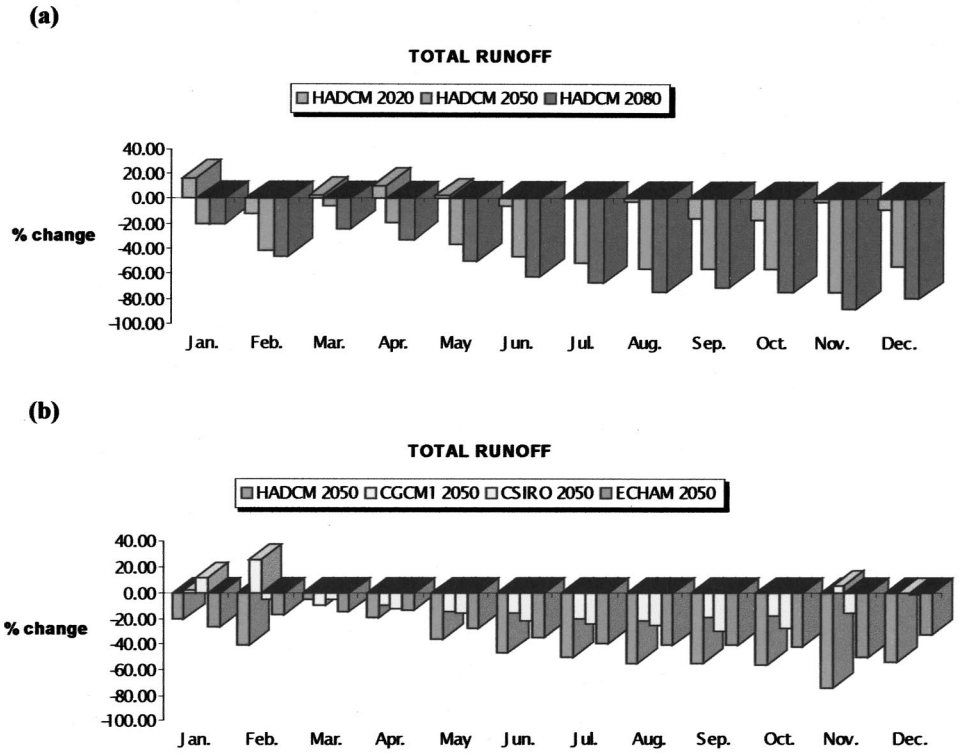

Fig. 16. Percentage changes of mean monthly total runoff: (a) first cluster of climate change scenarios; (b) second cluster of climate change scenarios

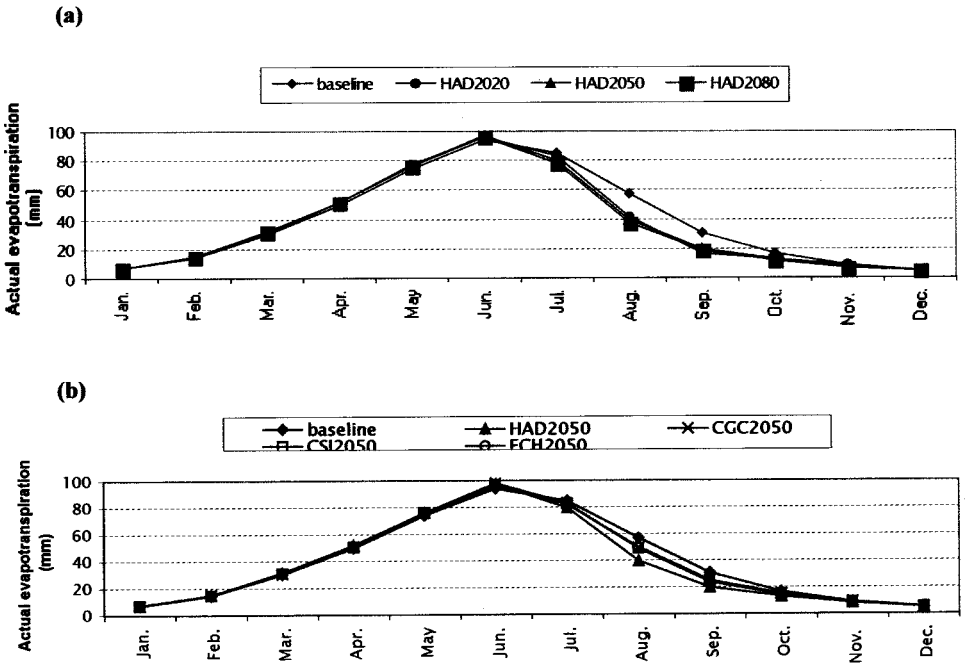

Fig. 17. Mean monthly evapotranspiration: (a) baseline and first cluster of climate change scenarios; (b) baseline and second cluster of climate change scenarios

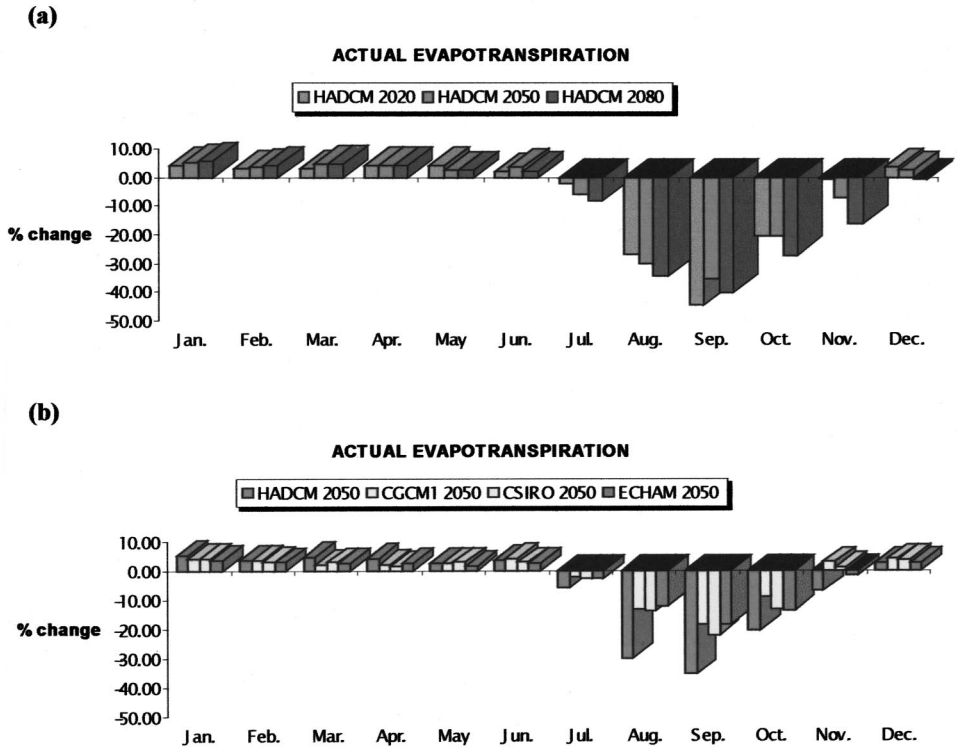

Fig. 18. Percentage changes of mean monthly evapotranspiration: (a) first cluster of climate change scenarios; (b) second cluster of climate change scenarios

Results and Discussion

Hydrological Balances

The methodology used to carry out the sensitivity study of the catchment consisted of running the SWAT model under climatically changed conditions and comparing the outputs to their baseline values. The impact on the monthly streamflow is illustrated by the analysis of the impact of climate change on its three components, which are the surface flow, the lateral flow, and the groundwater flow. The results are well in accordance with results of previous studies conducted in the same catchment (Mimikou et al. 1999a, 2000).

Surface Flow

The model simulates the surface flow as a function of precipitation. Thus, as expected, the changes in surface flow are according to the variation of the changes in precipitation, as given by the scenarios. Fig. 9 represents the mean monthly surface flow in the perturbed and baseline conditions. For all of the scenarios, the response of surface runoff to precipitation reduction is a decrease of the monthly values. Percentage changes (Fig. 10) can be as high as 90% reduction, as in the case of the HadCM 2050 scenario for the surface flow in August.

Lateral Flow

The reduction in lateral flow is more straightforward and characteristic of the reduced soil moisture in the catchment. Reduction is observed for all months and all scenarios (Fig. 11). The highest reduction (Fig. 12) is given by the HadCM 2080 scenario, which suggests the drier conditions.

Groundwater Flow

Groundwater runoff is the steadiest of all of the constituent parts of total runoff. In general, because of the variability of soil con-

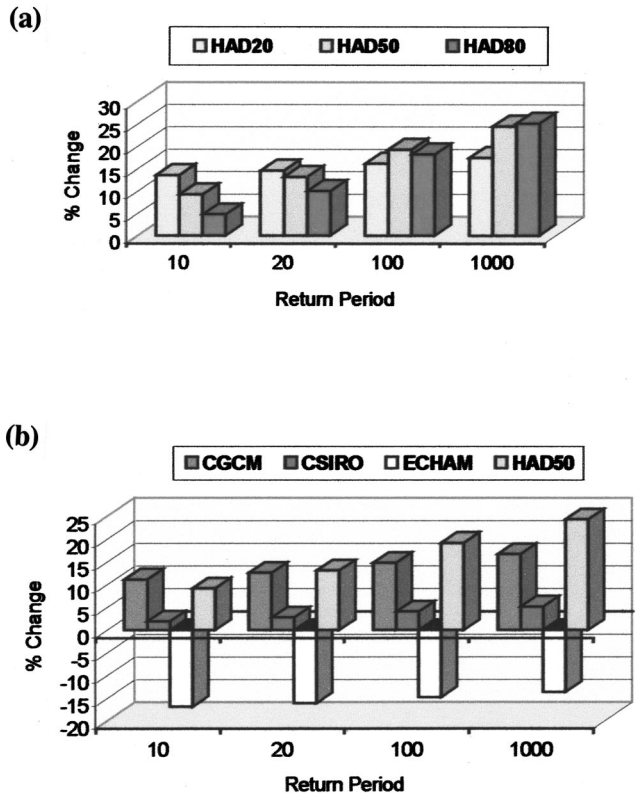

Fig. 19. Percentage changes of 10, 20, 100, and 1,000 year floods: (a) first cluster of climate change scenarios; (b) second cluster of climate change scenarios

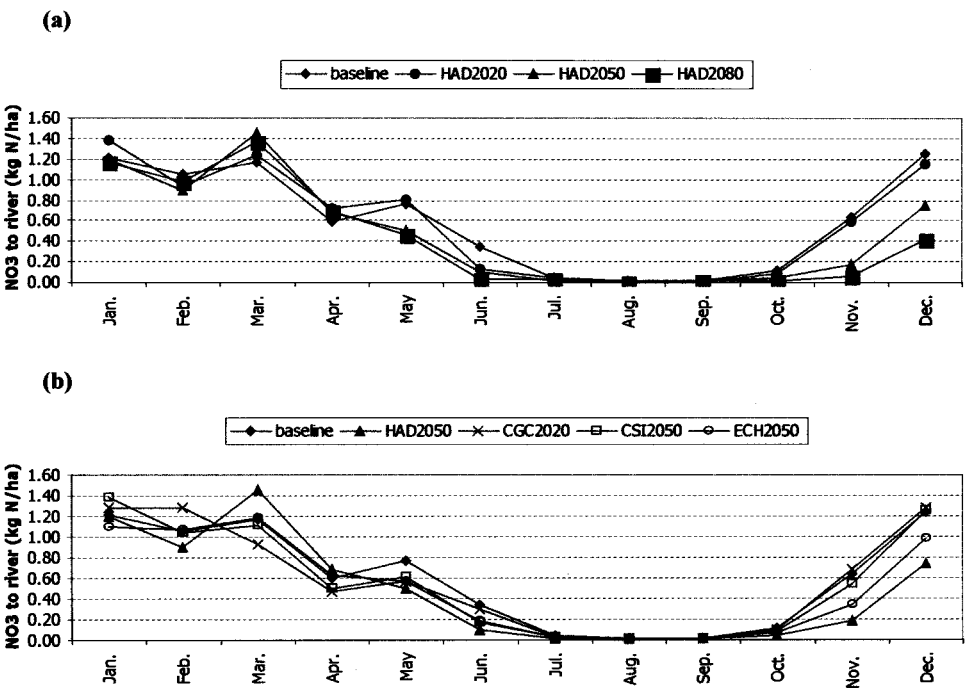

Fig. 20. Mean monthly nitrate nitrogen losses: (a) baseline and first cluster of climate change scenarios; (b) baseline and second cluster of climate change scenarios

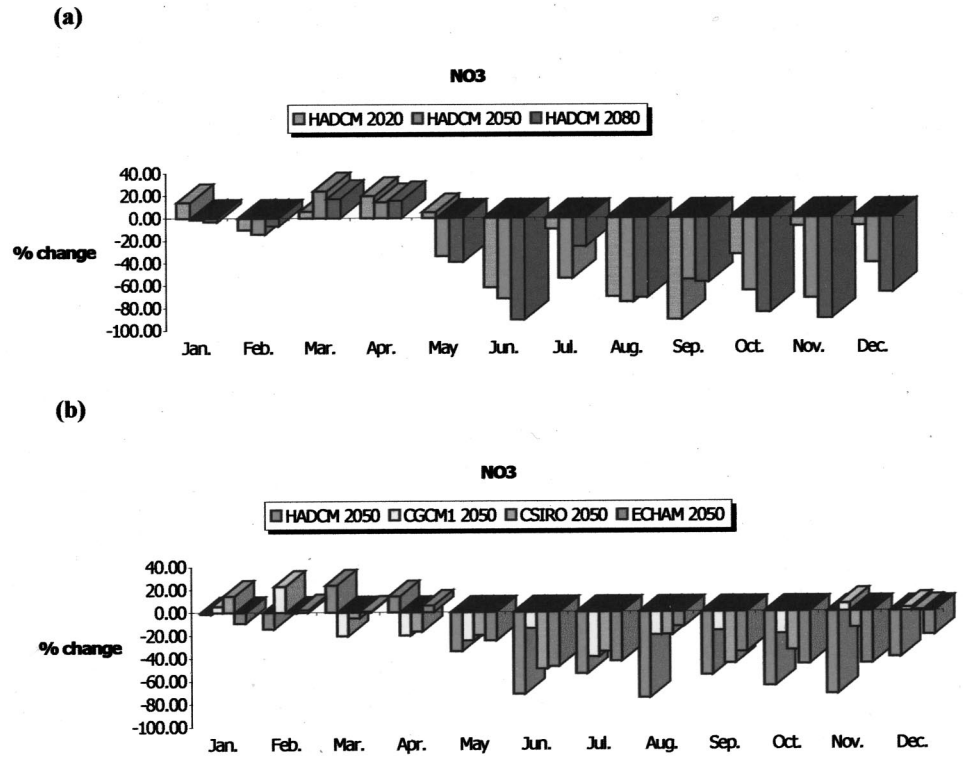

Fig. 21. Percentage changes of mean monthly nitrate nitrogen loss: (a) baseline and first cluster of climate change scenarios; (b) baseline and second cluster of climate change scenarios

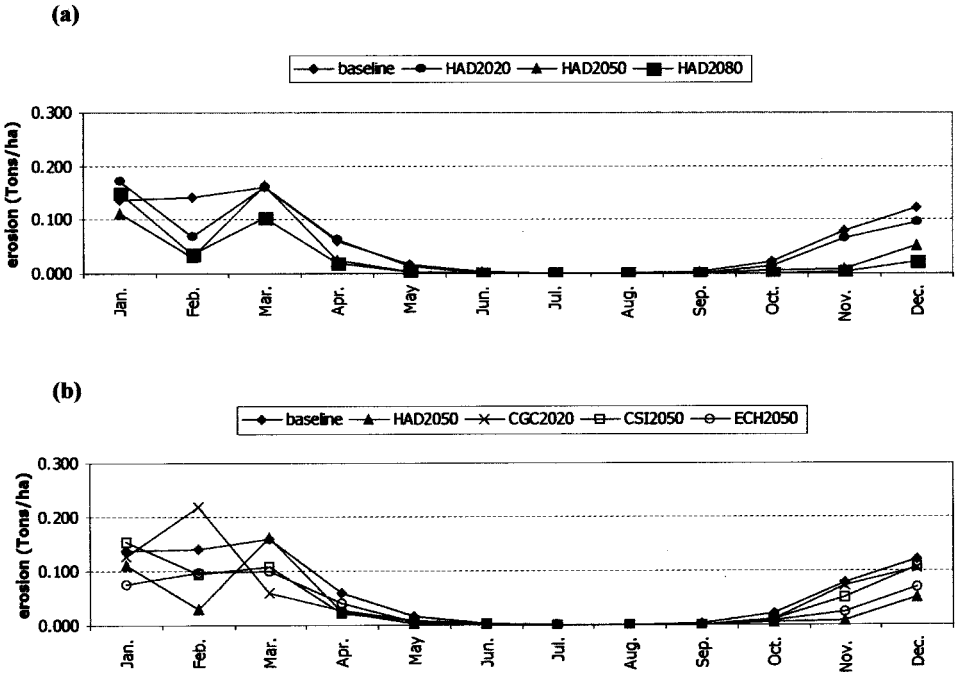

Fig. 22. Mean monthly sediment losses: (a) baseline and first cluster of climate change scenarios; (b) baseline and second cluster of climate change scenarios

ditions, the effect of a given amount of precipitation on groundwater flow is not always straightforward. However, in the current study, the decrease in groundwater flow throughout the year, as can be seen in Fig. 13, is pronounced, for all scenarios. Again, the highest reduction is observed for the HadCM 2080 scenario (Fig. 14).

Total Runoff

The impact of climate change on the total runoff is subsequent to the impacts on the constituent parts described above. It has been estimated that there will be a significant decrease of the mean monthly runoff for almost all months (Fig. 15) as a result of a warmer and drier future. It is important that the decrease (Fig. 16)

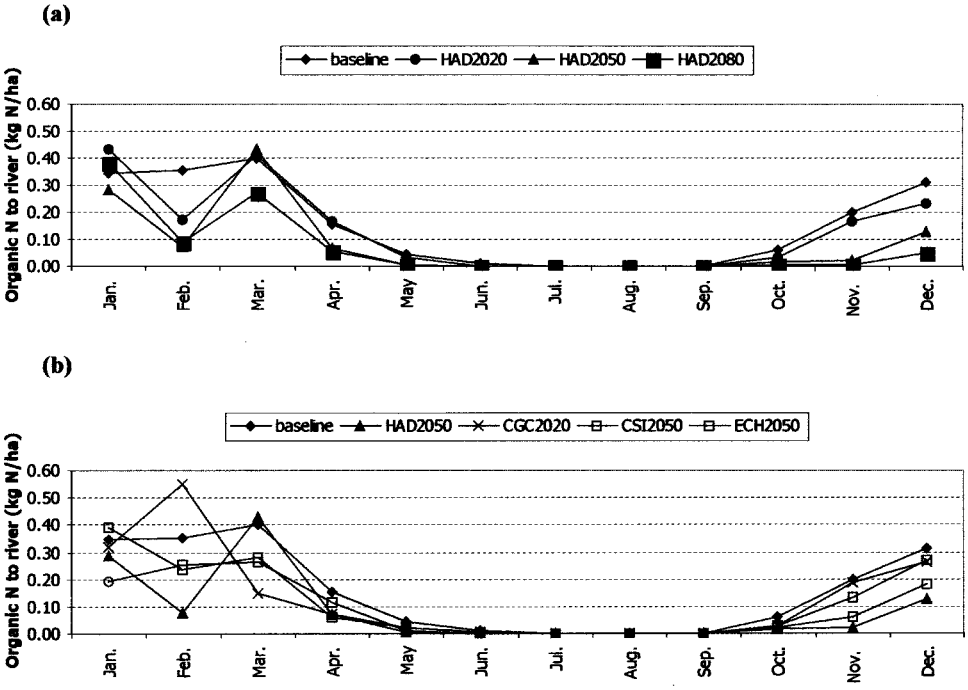

Fig. 23. Mean monthly organic nitrogen losses: (a) baseline and first cluster of climate change scenarios; (b) baseline and second cluster of climate change scenarios

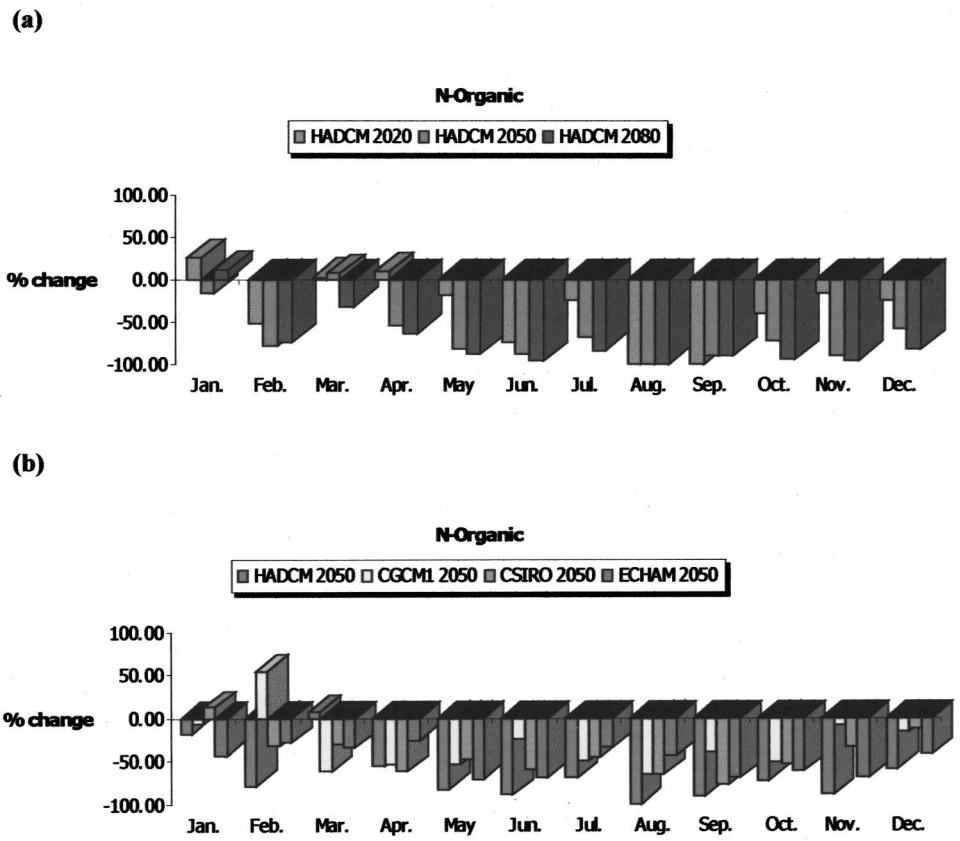

Fig. 24. Percentage changes of mean monthly organic nitrogen loss: (a) baseline and first cluster of climate change scenarios; (b) baseline and second cluster of climate change scenarios

is high in October and November for both clusters of scenarios, resulting in a prolonged drought period, with serious implications for water management practices.

Actual Evapotranspiration

In general, there are no remarkable up trends or down trends in actual evapotranspiration, with the exception of the months of August to November (Fig. 17). The reduction of actual evapotranspiration as can be seen in Fig. 18 is pronounced during those months, for both clusters of scenarios. The dry soil moisture conditions during the summer explain the reduction of actual evapotranspiration in the specific months. Similar results have been observed in other Greek catchments (Mimikou et al. 1999b).

Floods

Another component of the study is to analyze the impact of climate change on flood magnitude. The Gumbel maximum distribution has been fitted to the annual daily maxima of the 30 year runoff series, for the baseline and for all of the scenarios. The 10, 20, 100, and 1,000 year floods have been estimated for all scenarios of the two clusters. The changes in flood magnitude for the first cluster [Fig. 19(a)] indicate an increase that can be as high as 20% for the 1,000 year flood of the HadCM 2080 scenario (Knox 1993). However, in the second cluster [Fig. 19(b)], results for the ECHAM scenario behave exceptionally and indicate a decrease of the flood magnitude. This is mainly due to the different percentage of precipitation decrease that the certain scenario suggests and due to the number of wet days on which those changes were perturbed. Additionally, the different scenarios are a combination of different percentages of precipitation reduction and temperature increase, meaning that one has to look with caution at the magnitude of change on both variables, precipitation and temperature. Those results indicate that the cause-effect relationship with regard to climate change remains a difficult issue. Climate change scenarios are scenarios of the future, and thus any impact study is inherently uncertain (Mimikou 1995; Pielke and Downton 2000).

Nitrogen Losses

Nitrate losses depend on the hydrological balance, the quantity of nitrogen present in the soil either from natural sources (organically bound nitrogen, nitrogen from fixation, and atmospheric deposition) or fertilizer input, and the degree to which nitrogen is removed by plants at the site (Ferrier et al. 1995). The impact of these factors varies for each site.

The climate change impact on nitrate nitrogen losses is depicted in Figs. 20(a and b). According to the simulations, changes in precipitation have a pronounced effect on the nitrate nitrogen losses. Elevated nitrate nitrogen losses are expected during the spring, when most of the fertilizer applications take place and the climate scenarios predict increased runoff. High temperatures are in favor of mineralization, and increased nitrate concentrations would be expected during autumn as a result of residue decomposition. However, decreased surface and lateral flows result in reduced nitrate losses. The percentage changes for both of the climate change scenario clusters are depicted in Figs. 21(a and b). Decreasing water discharge appeared to be the most significant factor in dropping the inorganic nitrogen runoff also in the studies of Mander et al. (1998, 2000).

The model simulates organic N transport as a function of organic N in the topsoil layer, the sediment yield, and the ratio of organic nitrogen concentration attached to the sediments divided by the organic nitrogen concentration in the soil. Therefore, erosion change patterns [Figs. 22(a and b)] affect the organic nitrogen losses [Figs. 23(a and b)]. Erosion changes themselves follow the surface runoff changes (Fig. 10).

For the first cluster of scenarios, radical changes with respect to organic nitrogen losses are expected according to HadCM 2080. The second cluster of scenarios, and especially HadCM 2050, predict significant reductions, while CGCM1 2050 predicts a 60% increase for February (Fig. 24).

Conclusions

The main conclusions drawn from this environmental impact assessment study can be summarized into the following points:

- Although the climate change scenarios used in the study are outputs of different GCMs and are for different time slices, all exhibit a warmer and drier future for the study area, resulting in reduced monthly total runoff,
- There are no significant changes in the actual evapotranspiration, with the exception of the summer months, when the dry soil conditions result in a decrease of the variable,
- Climate has an important, but by no means determining, role in the growth of floods. The uncertainty while moving in a finer time scale (daily) is still large, and the use of different GCM outputs and simple downscaling procedures can lead to adverse results. However, there is evidence of increasing flood magnitude,
- Reduced losses for both nitrate and organic nitrogen are observed for all of the months for which the scenarios predict reduced precipitation, and
- Changes in precipitation have a pronounced effect on nitrogen losses as a result of both surface runoff and erosion changes.

Acknowledgments

This research has been supported by the Environment and Climate Research Program of the EU, DGXII, in the framework of contracts ENV4-CT97-0535 (EUROTAS) and ENV4-CT97-0440 (CHESS).

References

Arnell, N. W. (1998). ''The effect of climate change on hydrological regimes in Europe: A continental perspective.'' *Global Environ. Change*, 9, 5–23.

Arnold, J. G., Muttiah, R. S., Srinivasan, R., and Allen, P. M. (2000). ''Regional estimation of base flow and groundwater recharge in the Upper Mississippi River basin.'' *J. Hydrol.*, 227, 21–40.

Arnold, J. G., Williams, J. R., Srinisavan, R., and King, K. W. (1994). ''SWAT: Soil and water assessment tool.'' U.S. Dept. of Agriculture, Agricultural Research Service, Temple, Tex.

Cullen, M. J. P. (1993). ''The unified forecast/climate model.'' *Meteorol. Mag.*, 122, 81–95.

Danalatos, N. G. (1992). ''Quantified analysis of selected land use systems in the Larissa region, Greece.'' Doctoral thesis, Agricultural Univ., Wageningen, Greece.

Ferrier, R. C., Whitehead, P. G., Sefton, C., Edwards, A. C., and Pugh, K. (1995). ''Modelling impacts of land use change and climate change on nitrate-nitrogen in the River Don, North East Scotland.'' *Water Res.*, 29, 1950–1956.

Flato, G. M., et al. (1999). ''The Canadian Centre for Climate Modelling and Analysis global coupled model and its climate.'' *Clim. Dyn.*, in press.

Hirst, A. C., Gordon, H. B., and O'Farrell, S. P. (1996). ''Global warming in a coupled climate model including oceanic eddy-induced advection.'' *Geophys. Res. Lett.*, 23, 3361–3364.

Hirst, A. C., O'Farrell, S. P., and Gordon, H. B. (1999). ''Comparison of a coupled ocean-atmosphere model with and without oceanic eddy-induced advection. 1. Ocean spinup and control integrations.'' *J. Clim.*, in press.

Hulme, M., Barrow, E., Arnell, N., Harrison, P., Johns, T., and Downing, T. (1999). ''Relative impacts of human-induced climate change and natural climate variability.'' *Nature (London)*, 397, 688–691.

Johns, T. C. et al. (1997). ''The Second Hadley Centre coupled ocean-atmosphere GCM: Model description, spinup and validation.'' *Clim. Dyn.*, 13, 103–134.

Knox, J. C. (1993). ''Large increases in flood magnitude in response to modest changes in climate.'' *Nature (London)*, 361, 423–425.

Krysanova, V., Müller-Wohlfeil, D. I., and Becker, A. (1998). ''Development and test of a spatial distributed hydrological/water quality model for mesoscale watersheds.'' *Ecologic. Model.*, 106, 261–289.

Mander, Ü., Kull, A., Kuusemets, V., and Tamm, T. (2000). ''Nutrient runoff dynamics in a rural catchment: Influence of land-use changes, climatic fluctuations and ecotechnological measures.'' *Ecological Eng.*, 14, 405–417.

Mander, Ü., Kull, A., Tamm, V., Kuusemets, V., and Karjus, R. (1998). ''Impact of climatic fluctuations and land use change on runoff and nutrient losses in rural landscapes.'' *Landscape Urban Plan.*, 41, 229–238.

Mimikou, M. A. (1995). ''Climate change.'' *Environmental hydrology*, V. P. Singh, ed., Kluwer Academic, Boston, 69–106.

Mimikou, M. A., Baltas, E., Varanou, E., and Pantazis, K. (1999a). ''Impacts of climate change on the water resources quantity and quality.'' *Proc., Int. Conf. on Water, Environment, Ecology, Socio-economics, and Health Engineering*.

Mimikou, M. A., Baltas, E., Varanou, E., and Pantazis, K. (2000). ''Regional impacts of climate change on water resources quantity and quality indicators.'' *J. Hydrol.*, in press.

Mimikou, M. A., Hadjissava, P., Kouvopoulos, Y., and Afrateos, H. (1991b). ''Regional climate change impacts. II. Impacts on water management works.'' *Hydrol. Sci. J.*, 36, 259–270.

Mimikou, M. A., Kanellopoulou, S., and Baltas, E. (1999b). ''Human implication of changes in the hydrological regime due to climate change in Northern Greece.'' *Global Environ. Change*, 9, 139–156.

Mimikou, M., and Kouvopoulos, Y. (1991). ''Regional climate change impacts. I. Impacts on water resources.'' *Hydro. Sci. J.*, 36, 247–258.

Mimikou, M., Kouvopoulos, Y., Cavvadias, G., and Vayiannos, N. (1991a). ''Regional hydrological effects of climate change.'' *J. Hydrol.*, 123, 119–146.

Ministry of the Environment, Physical Planning and Public Works. (1998). ''Long-term water quality data of Pinios River, period 1988–1998: Raw data.'' (in Greek).

Nash, J. E., and Sutcliffe, J. V. (1970). ''River flow forecasting through conceptional models. I. A discussion of principles.'' *J. Hydrol.*, 10, 282–290.

National Statistical Service of Greece. (1997). ''Agricultural statistics of Greece.''

Neitsch, S. L., Arnold, J. G., and Williams, J. R. (1999). *Soil and water assessment tool: User's manual—Version 98.1*, Agricultural Research Service, Temple, Tex.

Pielke, R. A., and Downton, M. W. (2000). ''Precipitation and damaging floods: Trends in the United States, 1932–1997.'' *J. Clim.*, in press.

Roeckner, E., et al. (1996). ''The atmospheric general circulation model ECHAM-4: Model description and simulation of present-day cli-

mate.'' *Rep. No. 218*, Max-Planck Institute for Meteorology, Hamburg, Germany.

Skop, E., and Sørensen, P. B. (1998). ''GIS-based modelling of solute fluxes at the catchment scale: A case study of the agricultural contribution to the riverine nitrogen loading in the Vejle Fjord catchment, Denmark.'' *Ecologic. Model.*, 106, 291–310.

Univ. of Patras. (1999). ''Vulnerable zones of Greece due to nitrate pollution resulting from agricultural activities (in application of the Directive 91/6767/EEC).'' *Final Rep., Prepared for Ministry of the Environment, Physical Planning and Public Works*, Dept. of Geology, Hydrogeology Laboratory, Patras, Greece.